

Results of the TWIST blind analysis

G.M. Marshall, for the TWIST Collaboration^a

TRIUMF, 4004 Wesbrook Mall, Vancouver, British Columbia, Canada V6T 2A3

After a decade of design, construction, improvement, data-taking, simulation, and analysis, the TRIUMF Weak Interaction Symmetry Test (TWIST) muon decay parameter measurement is nearly complete. Results of the blind analysis are now available. While there are still some subtle systematic effects that preclude final values of the decay parameters ρ , δ , and $\mathcal{P}_\mu^\pi \xi$, the goal of an order-of-magnitude improvement on pre-TWIST precisions appears to have been achieved.

1 Introduction

The decay of polarized muons ($\mu \rightarrow e \nu \bar{\nu}$), where neither the electron polarization nor the accompanying neutrinos are observed, can be described by the differential rate as^{1,2,3}

$$\frac{d^2\Gamma}{dx d\cos\theta} = \frac{1}{4}m_\mu W_{\mu e}^4 G_F^2 \sqrt{x^2 - x_0^2} \cdot \{\mathcal{F}_{IS}(x, \rho, \eta) + \mathcal{P}_\mu \cos\theta \cdot \mathcal{F}_{AS}(x, \xi, \delta)\}$$

with

$$W_{\mu e} = \frac{m_\mu^2 + m_e^2}{2m_\mu}, \quad x = \frac{E_e}{W_{\mu e}}, \quad x_0 = \frac{m_e}{W_{\mu e}}, \quad \mathcal{P}_\mu = |\vec{\mathcal{P}}_\mu|, \quad \cos\theta = \frac{\vec{\mathcal{P}}_\mu \cdot \vec{p}_e}{|\vec{\mathcal{P}}_\mu| |\vec{p}_e|}$$

$$\begin{aligned} \mathcal{F}_{IS}(x, \rho, \eta) &= x(1-x) + \frac{2}{9}\rho(4x^2 - 3x - x_0^2) + \eta x_0(1-x) \\ \mathcal{F}_{AS}(x, \xi, \delta) &= \frac{1}{3}\sqrt{x^2 - x_0^2} \left[1 - x + \frac{2}{3}\delta \left\{ 4x - 3 + \left(\sqrt{1 - x_0^2} - 1 \right) \right\} \right] \end{aligned}$$

The neutrino mass is neglected. Radiative corrections are not explicitly shown, but are significant and must be evaluated within the standard model (SM) to a precision compatible with the experiment. The isotropic term $\mathcal{F}_{IS}(x)$ depends on the decay parameters ρ and η , while the asymmetric part $\mathcal{F}_{AS}(x)$ depends on δ and ξ . The asymmetric part is multiplied by the polarization of the muon at the time of decay, \mathcal{P}_μ , which may evolve over the 2.2 μ s mean lifetime of the muon from the polarization \mathcal{P}_μ^π at the time of the muon's birth, e.g., in pion decay at rest. The TRIUMF Weak Interaction Symmetry Test (TWIST) has been constructed

^a <http://twist.triumf.ca/>: R. Bayes, Yu.I. Davydov, W. Faszer, M.C. Fujiwara, A. Grossheim, D.R. Gill, P. Gumplinger, A. Hillaire, R.S. Henderson, J. Hu, G.M. Marshall, R.E. Mischke, K. Olchanski, A. Olin, R. Openshaw, J.-M. Poutissou, R. Poutissou, G. Sheffer, B. Shin (TRIUMF), A. Gaponenko, R.P. MacDonald (University of Alberta), J.F. Bueno, M.D. Hasinoff (University of British Columbia), P. Depommier (Université de Montréal), E.W. Mathie, R. Tacik (University of Regina), V. Selivanov (Russian Research Center, Kurchatov Institute), C.A. Gagliardi, R.E. Tribble, (Texas A&M), D.D. Koetke, T.D.S. Stanislaus (Valparaiso University).

to determine the Michel parameter ρ as well as the parameters δ and $\mathcal{P}_\mu^\pi \xi$ with a precision approximately one order of magnitude better than prior experiments, as a test of the SM.

Prior to 1990, the three decay parameters were known with uncertainties in the range of 3.5-8.5 parts per thousand. Intermediate TWIST results have already reduced those uncertainties to 0.7-3.8 parts per thousand.^{4,5} The decay parameters measured by TWIST contribute to a larger set derived from other observables that can be analyzed in terms of a generalized matrix element containing scalar, vector, and tensor interactions for muons and electrons of left and right chirality.^{6,7} A global analysis^{4,8} reveals consistency with the standard model, where the vector coupling for muons and electrons of left-handed chirality is the only non-zero term. The results from TWIST restrict the upper limits of other terms, especially those for left-handed electrons and right-handed muons. For example, the probability for right-handed muon couplings in muon decay was reduced by a factor of two to less than 2.4×10^{-3} (90% confidence).

2 Experimental details

The TWIST spectrometer is shown in Fig. 1. The data-taking phase of the experiment was completed in 2007. Highly polarized positive muons were selected from decays of stationary pions at the surface of a graphite production target. They were guided into the superconducting solenoidal field along its symmetry axis to enter a high-precision, low-mass stack of proportional and drift chambers.⁹ The muons were ranged to stop predominantly in a high-purity metal foil at the center of the symmetric stack. Data sets were taken with two foil stopping targets, silver (thickness $30.9 \mu\text{m}$) and aluminum (thickness $71.6 \mu\text{m}$). Tracks from decay positrons in the uniform, precisely known 2 T field were sampled by the low-mass drift chambers in a helium gas environment. Analysis provides two-dimensional distributions of positron angle and momentum (or energy) whose shape depends on the decay parameters. With a muon rate of order $2\text{--}5 \times 10^3 \text{ s}^{-1}$, data sets of 10^9 events could be obtained in a few days. Approximately 3% of events pass event and track selection criteria as well as fiducial cuts on energy and angle. Much care is taken to test for and avoid the introduction of any bias. The fiducial cuts are symmetric for upstream and downstream decays, and are selected to maximize sensitivity to the decay parameters while reducing systematic uncertainties.

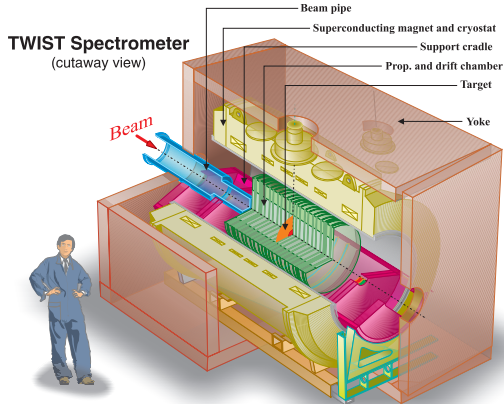


Figure 1: The TWIST spectrometer.

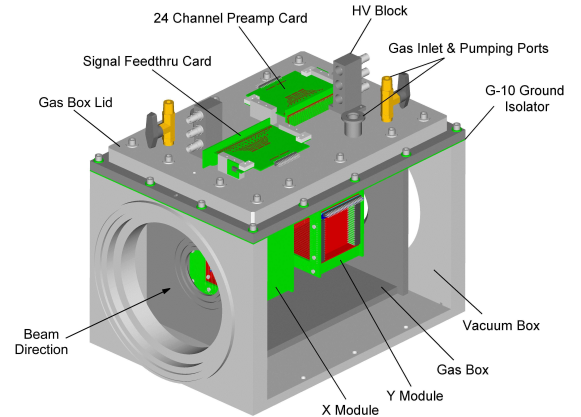


Figure 2: The TWIST TECs.

To determine the incoming muon beam characteristics (size, position, divergence, and correlations), a beam monitor detector was inserted to measure the beam before it entered the solenoid (see Fig. 2). This detector is a pair of time expansion chambers (TECs) recording the position and angle of each incident muon.¹⁰ Because they caused multiple scattering and hence

muon depolarization, the TECs were typically removed for precise decay measurements, but the beam characteristics measured between data sets formed an essential input to the simulation and analysis of decay data.

3 Analysis procedures

The important principle of TWIST analysis is the comparison of energy-angle two-dimensional distributions of data to similar ones derived from a GEANT3 simulation. Both are subjected to essentially the same analysis, allowing bias and inefficiencies to be included in an equivalent way to reduce the dependence of the result on the specific analysis procedure. This places great importance on the accuracy and detail of the simulation, which includes not only standard physics processes but also a detailed description of the beam, magnetic field, geometry, and detector response. Decay parameters are obtained by a “blind” fit of the two-dimensional data distribution to that of a base distribution of simulated events, generated with hidden muon decay parameters, plus distributions corresponding to the two-dimensional spectrum shape of first derivatives of the spectrum with respect to decay parameters (or combinations) ρ , ξ , and $\xi\delta$, also derived from simulated events.

4 Systematic uncertainties

The procedure of fitting the difference of two spectra in terms of derivatives also plays a key role in evaluation of systematic uncertainties, by finding the effect on the decay parameters when an identified source of systematic uncertainty is changed (often by an exaggerated amount) in one of the spectra. This is most commonly achieved with two simulated spectra. The systematic contributions as determined prior to revealing the hidden parameters of the blind analysis are listed, along with statistical uncertainties, in Table 1.

Table 1: Systematic and statistical uncertainties for ρ , δ , and $\mathcal{P}_\mu^\pi \xi$ prior to revealing hidden parameters.

Uncertainties	$\rho(\times 10^{-4})$	$\delta(\times 10^{-4})$	$\mathcal{P}_\mu^\pi \xi(\times 10^{-4})$
Positron interactions	1.8	1.6	0.7
Momentum calibration	1.2	1.2	1.5
Chamber response	1.0	1.8	2.3
External uncertainties	1.3	0.6	1.2
Resolution	0.6	0.7	1.5
Spectrometer alignment	0.2	0.3	0.2
Beam stability	0.2	0.0	0.3
Depolarization in fringe field			+15.8, -4.0
Depolarization in stopping material			3.2
Background muons			1.0
Depolarization in production target			0.3
<i>Total systematics in quadrature</i>	2.8	2.9	+16.5, -6.2
Statistical uncertainty	0.9	1.6	3.5
<i>Total uncertainty</i>	3.0	3.3	+16.9, -7.2

Four sources dominate for ρ and δ : positron interactions, momentum calibration, chamber response, and external uncertainties due to radiative corrections and the assumed value of η . The first three were improved substantially compared to our intermediate results.⁴ The positron interactions systematic relates the possible inaccuracy in our simulation of reproducing positron energy loss in the stopping target and detector elements, due primarily to bremsstrahlung,

delta-ray production, and ionization. It was better constrained by comparisons of identified interactions observed in the data and in the simulation. Chamber response refers to the conversion of drift chamber time information to spatial information used in helix fitting and evaluation of the momentum and angle of each track. It was improved by more precise monitoring and control of atmospheric influences that could change chamber cell geometry. In addition, a method was developed¹¹ by which the detector space-time relations (STRs) were modified for each plane to minimize positron decay track fit residuals. The tracking bias was reduced by applying the procedure also to simulations. Changes to the spatial isochrone shapes varied from zero to $\sim 40 \mu\text{m}$ in drift cells of $4 \times 4 \text{ mm}^2$. The maximum positron energy provides a calibration feature that is used to reduce the energy scale systematic. Since energy loss depends on the track angle primarily with a dependence on $1/(\cos \theta)$ due to the planar geometry of the detector, the energy region near the kinematic endpoint of $52.8 \text{ MeV}/c$ is matched for data and simulation for small bins of $\cos \theta$. The data-simulation relative energy calibration procedure has undergone improvements to become more robust to fitting conditions.

The asymmetry parameter ξ is also subject to uncertainties from these sources, but they are overshadowed by other unique uncertainties related to depolarization, as shown in Table 1. Depolarization in the fringe field and in the muon stopping target result in $\mathcal{P}_\mu < \mathcal{P}_\mu^\pi$, comprising the largest contributions to systematic uncertainties for $\mathcal{P}_\mu^\pi \xi$. They were also considerably improved for this analysis compared to the intermediate result.⁵ Fringe field depolarization systematics depend on the accuracy with which the muon spin evolution can be simulated as the beam passes through significant radial field components at the solenoid entrance. The simulation in turn depends on two ingredients: an accurate field map, and precise knowledge of the position and direction of the muons in the beam. Depolarization in the stopping target from muon spin relaxation ($\mu^+\text{SR}$) as the spins interact with the target material is assessed from the measured time dependence of the asymmetry.

5 Results

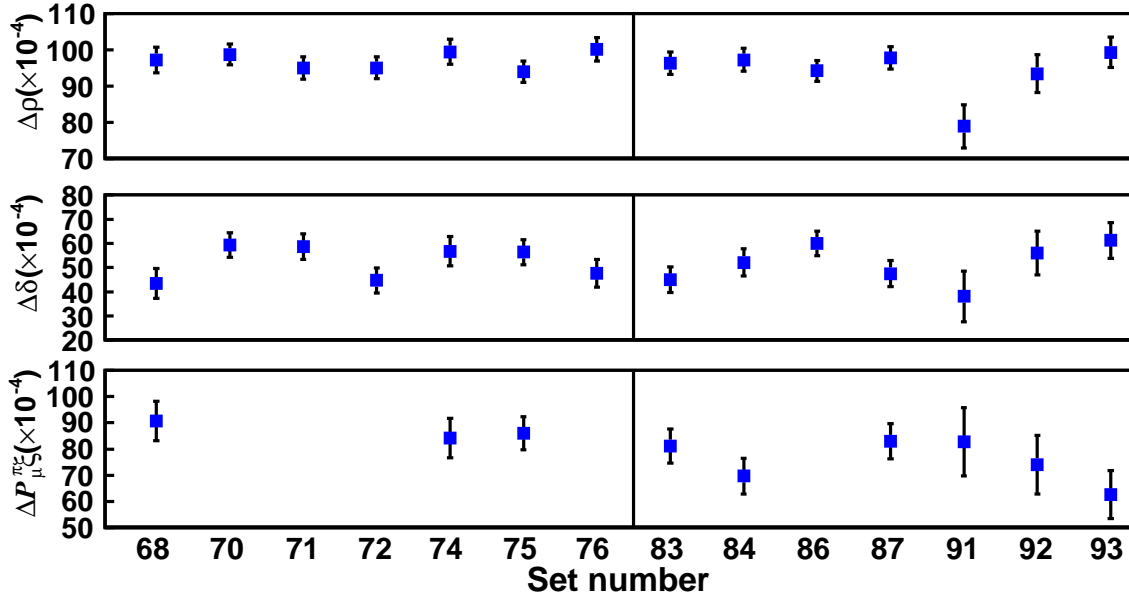


Figure 3: Comparison of fit results (differences of measured and hidden parameters) for data sets used in analysis. Only statistical uncertainties are shown, and small set-dependent systematic corrections have been applied. The vertical line divides sets obtained with targets of Ag (left) and Al (right).

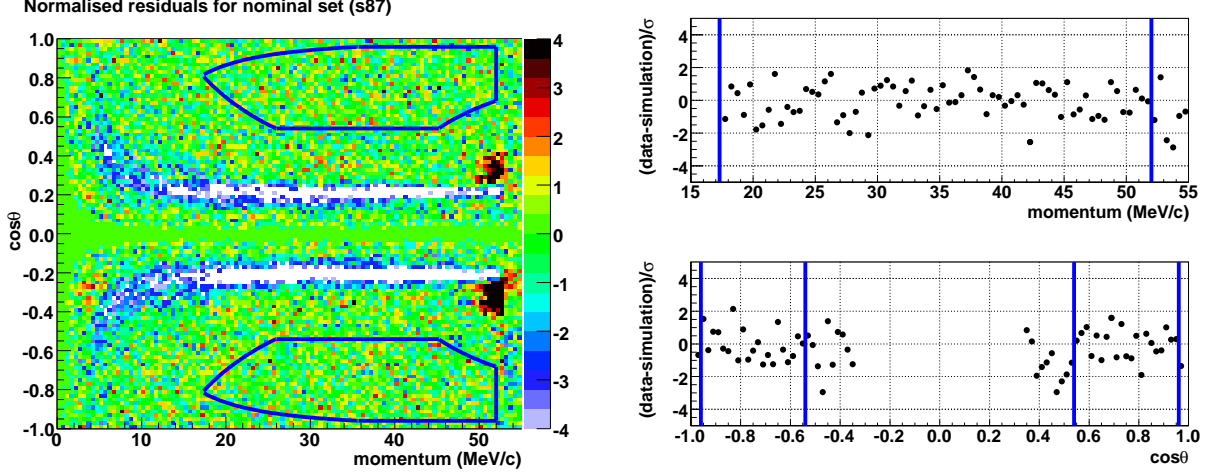


Figure 4: Comparison of data with a fit to simulation in terms of normalized residuals for one data set. The left plot is the entire range in momentum and $\cos\theta$, while the right plot shows projections of data within the fiducial (indicated by the solid line) onto the two axes.

Fourteen data sets were used to extract decay parameters ρ and δ , seven with each of the Ag and Al targets. Only nine sets were used for $\mathcal{P}_\mu^\pi \xi$; the other five were deemed to have poorly controlled polarization systematic uncertainties. The fringe field was not well measured for sets 70 (1.96 T field) and 71 (2.04 T field), there was added multiple scattering and thus increased fringe field depolarization for set 72 (TECs in place), while sets 76 and 86 were intentionally mis-steered to evaluate depolarization systematics in the fringe field. Fits to constant means for the difference values of Fig. 3 give reduced χ^2 values of 14.0/13 (ρ), 17.7/13 (δ), and 9.7/8 ($\mathcal{P}_\mu^\pi \xi$) respectively.

A visualization of the fit of one data set (set 87) in terms of residuals is shown in Fig. 4. It also shows an outline of the range of $(p, \cos\theta)$ used to determine the decay parameters. The limits of this fiducial range in momentum (total, transverse, and longitudinal) and angle are those within which the systematic biases and uncertainties are considered to be well controlled. For all fourteen data sets, there were 11×10^9 events, of which 0.55×10^9 passed event selection criteria and were within this fiducial range. Simulation data sets were about 2.7 times larger on average.

After revealing the hidden parameters, the results for the three decay parameters were:

$$\begin{aligned}\rho &= 0.74991 \pm 0.00009(\text{stat}) \pm 0.00028(\text{syst}) \\ \delta &= 0.75072 \pm 0.00016(\text{stat}) \pm 0.00029(\text{syst}) \\ \mathcal{P}_\mu^\pi \xi &= 1.00084 \pm 0.00035(\text{stat}) \pm_{-0.00063}^{+0.00165}(\text{syst})\end{aligned}$$

These differ from SM predictions of 0.75, 0.75, and 1.0 by -0.3σ , $+2.2\sigma$, and $+1.2\sigma$ respectively. The results are compared graphically to prior published results in Fig. 5. Also plotted is the product $\mathcal{P}_\mu^\pi \xi \delta / \rho = 1.00192 \pm_{-0.00066}^{+0.00167}$ (with correlations taken into account). This product defines the asymmetry between $\cos\theta = \pm 1$ at the maximum decay positron energy, which is 1.0 in the SM. While the deviations from the SM that are allowed in the generalized matrix element treatment of Fetscher et al.⁶ do not constrain the sign of differences in ρ , δ , and ξ , the product is constrained to be not greater than 1.0. This apparent contradiction has initiated an ongoing reconsideration of potential systematic effects that might have been overlooked in the blind analysis. While no credible cause has yet been identified, we believe the resolution will be in terms of systematic effects. Thus we prefer not to consider the results of the blind analysis as

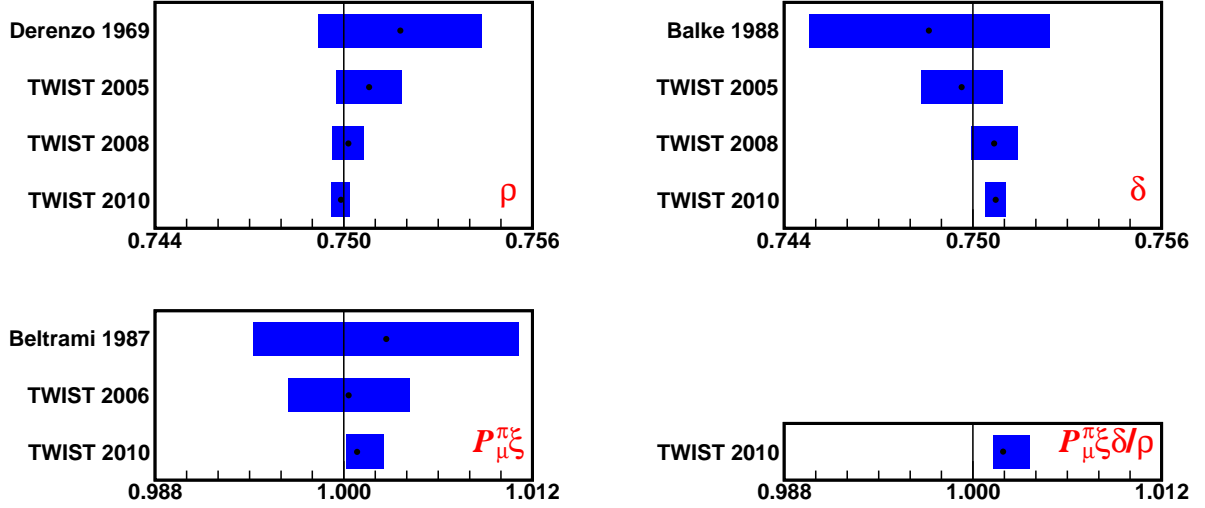


Figure 5: Summary of previously published values with uncertainties added in quadrature for three muon decay parameters, including those prior to TWIST, along with the results of this blind analysis. The combination $\mathcal{P}_\mu^{\pi\xi\delta/\rho}$ is also shown.

our final physics results, pending the outcome of a more complete re-assessment of potential sources of such effects.

6 Summary

We have achieved a substantial improvement for the final results of TWIST, compared to intermediate results and to prior experiments. Final checks of consistency and continuing re-evaluation of systematic uncertainties are underway, with the goal of understanding an apparent inconsistency in the product $\mathcal{P}_\mu^{\pi\xi\delta/\rho}$.

Acknowledgments

This work was supported in part by the Natural Sciences and Engineering Research Council (NSERC) of Canada, the U.S. Department of Energy, the Russian Ministry of Science, and by TRIUMF. High performance computing resources were provided by WestGrid (Canada).

References

1. L. Michel, *Proc. Phys. Soc.* **A63**, 514 (1950).
2. C. Bouchiat, and L. Michel, *Phys. Rev.* **106**, 170 (1957).
3. A. Sirlin, *Phys. Rev.* **108**, 844 (1957).
4. TWIST Collaboration, R.P. MacDonald, et al., *Phys. Rev. D* **78**, 032010 (2008).
5. TWIST Collaboration, B. Jamieson, et al., *Phys. Rev. D* **74**, 072007 (2006).
6. W. Fetscher, H.-J. Gerber, and K. F. Johnson, *Phys. Lett.* **B173**, 102 (1986).
7. Particle Data Group, C. Amsler, et al., *Physics Letters* **B667** (2008).
8. C. Gagliardi, et al., *Phys. Rev. D* **72**, 073002 (2005).
9. R. L. Henderson, et al., *Nucl. Instr. and Meth. A* **548**, 306 (2005).
10. J. Hu, et al., *Nucl. Instr. and Meth. A* **566**, 563 (2006).
11. A. Grossheim, et al., *Calibration of the TWIST high-precision drift chambers* (submitted to *Nucl. Instr. and Meth.*).